JOURNAL OF PHYSICAL ORGANIC CHEMISTRY
J. Phys. Org. Chem. 2006; **19:** 570–578
Published online 17 July 2006 in Wiley InterScience (www.interscience.wiley.com). DOI: 10.1002/poc.1060

The regiochemistry of the NO_3-promoted gas phase nitration of toluene and phenol with NO_2†

Ezio Bolzacchini,[1] Maurizio Bruschi,[1] Guido Galliani,[1] Jens Hjorth,[2] Marco Orlandi[1] and Bruno Rindone[1]*

[1]Dipartimento di Scienze dell'Ambiente e del Territorio, Universita' di Milano-Bicocca, Piazza della Scienza, 1, I-20126 Milano, Italy
[2]Joint Research Center, Ispra, Italy

Received 10 October 2005; revised 26 February 2006; accepted 3 March 2006

ABSTRACT: Product studies, kinetic isotope effect measurements, linear free energy relationships and calculations have been used to study the NO_3-promoted nitration of toluene and phenol in presence of NO_2. The competition between of a rate-determining hydrogen abstraction of NO_3 to give the benzyl radical and HNO_3 and of a rate-determining addition-elimination pathway has been evaluated. The preference for the nitration in *ortho* and *para* position of toluene and for the *ortho* position of phenol is suggested to derive from the concerted loss of nitric acid from an intermediate cyclohexadiene.A kinetic analysis suggests reasons for the dependence of the ratio *ortho*:*para*-nitration from the initial concentration of reactants. Copyright © 2006 John Wiley & Sons, Ltd.
Supplementary electronic material for this paper is available in Wiley Interscience at http://www.interscience.wiley.com/jpages/0894-3230/suppmat/

KEYWORDS: gas phase; nitration; nitrate radical; toluene; phenol; density functional theory

INTRODUCTION

Aromatic hydrocarbons such as benzene and toluene are one of the most important classes of primary pollutants emitted into the atmosphere from fuels and exhaust gases. This accounts for about 10% of all of the organic compounds in air. Functionalized aromatic compounds such as phenol can also be formed in the atmosphere by the OH-initiated atmospheric oxidation of these primary pollutants and their yields can be relatively high.[1,2] These aromatic compounds can subsequently be transformed into the corresponding nitroderivatives by reaction with NO_2 promoted by hydroxyl (OH) or nitrate (NO_3) radicals. These radicals are important oxidizing agents in the troposphere; the former during the day, the latter during the night.

The regiochemistry of the gas phase nitration of electron-rich aromatic compounds is often different from that in solution. Interestingly, there are also differences in OH- and NO_3-promoted nitrations, suggesting that different reaction pathways are involved in these two cases. Schemes 1 and 2 show three possible pathways in this reaction. They are:

1. A hydrogen abstraction reaction (H-ABS) forming a benzyl radical **6** ($X = CH_2$) or a phenoxy radical **6** ($X = O$). Addition of NO_2 will form *ortho*- and *para*-nitration products exclusively.
2. An electron transfer reaction (ET) to give a cation radical **7**. This is generally not occurring in gas phase chemistry.
3. An addition reaction (ADD) to give four isomeric adducts **2–5** in an equilibrium reaction. Addition of NO_2 gives seven isomeric cyclohexadienes **8–14**. These intermediates have generally two stereogenic carbons. Hence, a total of 24 isomers may be formed. These undergo elimination of HOY to give the three nitroderivatives **15–17**. Here, the nature of the cyclohexadiene intermediate controls the nitroderivative formed. Alternatively, loss of HOY from adducts **2–5** gives a benzyl radical **6** ($X = CH_2$) or a phenoxy radical **6** ($X = O$) with subsequent formation of *ortho*- and *para*-nitration products exclusively.

The gas phase OH-initiated nitration of toluene **1** ($X = CH_2$) with NO_2 has been extensively investigated both experimentally and theoretically. The rate of decay of OH with toluene shows an unusual dependence with the temperature.[3,4] At room temperature the OH decay is exponential and the rate constant decreases slightly with increasing the temperature giving a positive slope of the Arrhenius plot. In the range 325–380 K, the rate constant increases as a function of the temperature and the OH decay is no longer exponential. Finally, for temperatures above 380 K the rate constant increases as a function of

**Correspondence to:* B. Rindone, Dipartimento di Scienze dell' Ambiente e del Territorio, Universita' di Milano-Bicocca, Piazza della Scienza, 1, I-20126 Milano, Italy.
E-mail: Bruno.Rindone@unimib.it
†Selected paper presented at the 10th European Symposium on Organic Reactivity, 25–30 July 2005, Rome, Italy.
Contract/grant sponsor: EC; *contract/grant number:* ENV4-CT97-0411.

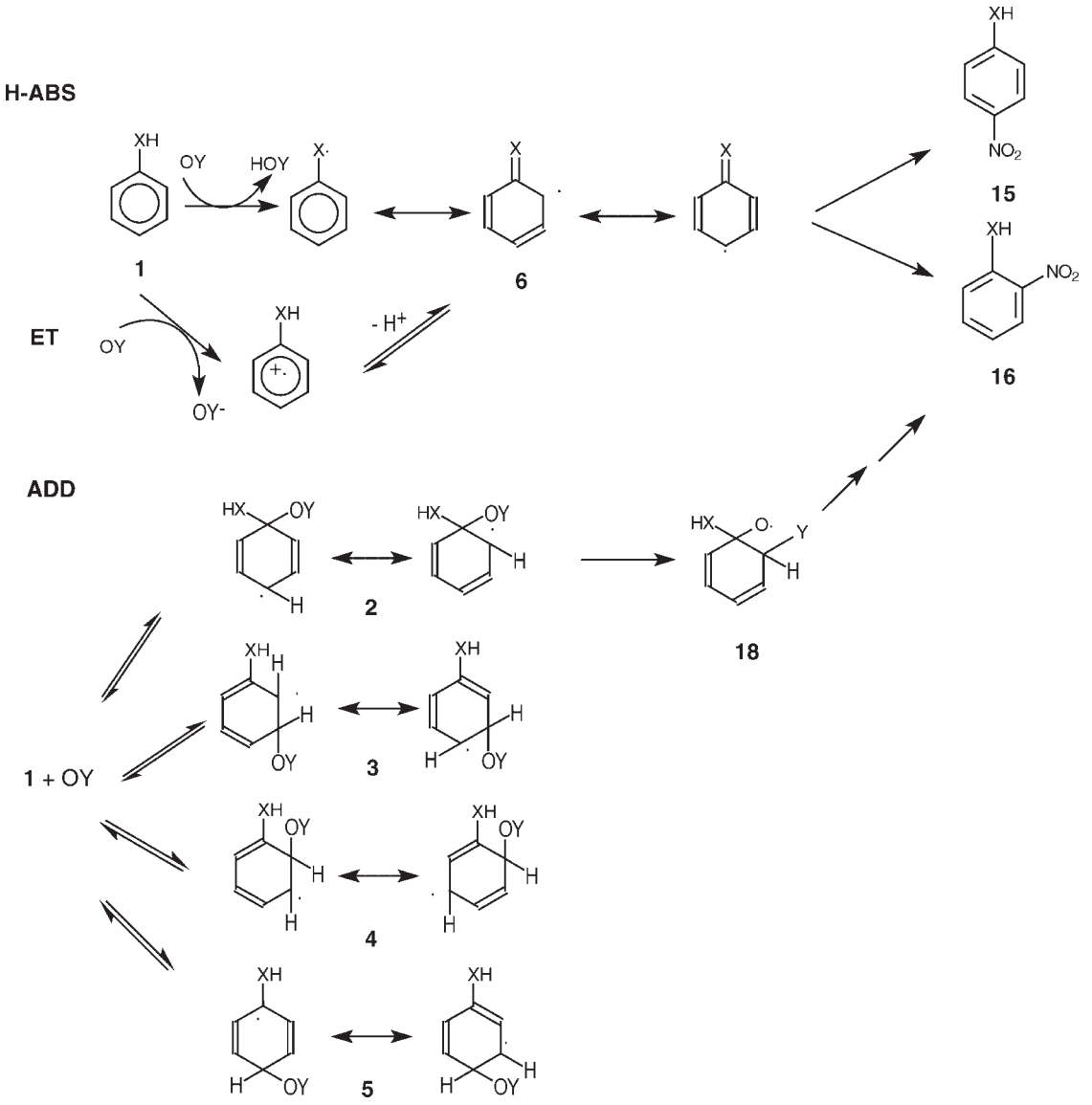

Scheme 1

the temperature but the OH decay is still exponential. The different behavior as a function of the temperature has been explained with the competition of the ADD and H-ABS mechanisms, which should be differently favored with the temperature. The negative activation energy observed at the room temperature (positive slope of the Arrhenius plot) has been explained with the formation of a OH-toluene pre-reactive complex with a (negative) binding energy larger than the subsequent (positive) activation energy to give the reaction products.[3–6] This pre-reactive complex has been characterized by Vivier-Bunge *et al*.[6]

In the OH-promoted nitration of toluene at room temperature, nitrotoluenes are formed in the ratio: *meta*:*para*:*ortho* = 70:25:5.[7,8] This ratio is very different from that observed in the electrophilic nitration of toluene in solution[9].

The reaction, at room temperature, is suggested to occur 90% via a rate-determining ADD giving at the equilibrium the predominant formation of the *ortho*-hydroxycyclohexadienyl radical adduct **4** ($X = CH_2$)[10] and 10% via a hydrogen abstraction reaction (H-ABS) which forms a benzyl radical **6** ($X = CH_2$). Accordingly, values of kinetic isotope effect (k_H/k_D) in the range 0.98–1.13 were found[11] and a Linear Free Energy Relationship (LFER) study[12] gave $\rho = -2.3 \pm 0.2$; $r^2 = 0.96$.

The H-ABS mechanism with toluene is reported to have higher k_H/k_D and lower ρ, for example, the bromination reaction ($k_H/k_D = 4.86 - 4.59$)[13], the chlorination with chlorine ($k_H/k_D = 3.6$–4.01,[14] $\rho = -1.5$[15]) or with hypochlorite ($k_H/k_D = 3.6$[16]; $\rho = -1.7$ against σ^+[14]), the microsomal oxidation ($k_H/k_D = 2.13$;[17] $\rho = -0.86$ against σ^+[18]).

The radical adducts reacts with O_2 in an equilibrium reaction[19] to give a peroxy radical and this is the reason for the predominant formation of *ortho*-cresol[20] together with other ring-retaining compounds[21] and ring fragmentation

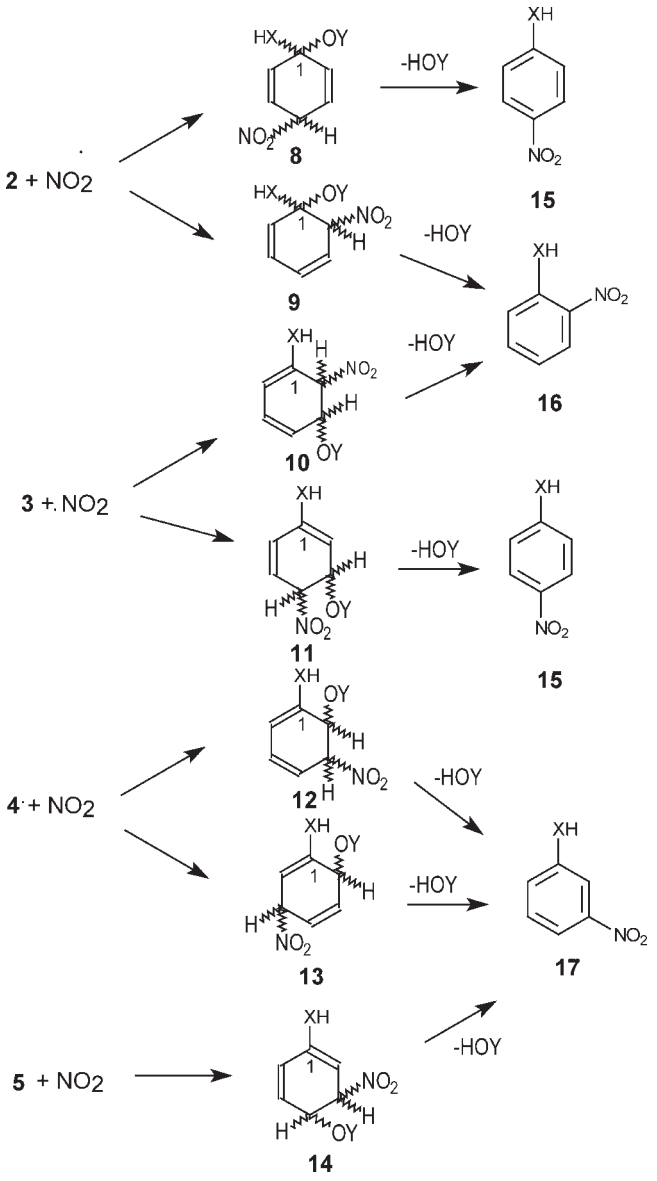

Scheme 2

products.[22] If NO_2 is present, in a competitive pathway the hydroxycyclohexadienyl radical adduct **4** (X = CH_2) will react with NO_2 to give cyclohexadienes **12–13** (X = CH_2)[23] A 1,2-elimination reaction of H_2O will form mainly 3-nitrotoluene **17** (X = CH_2).

The gas phase NO_3-initiated nitration of toluene and phenol has been less extensively investigated and the regiochemistry of the reaction is still far from being rationalized.

Prompted by these considerations we present in this work an experimental and computational study on the NO_3-initiated nitration of toluene and phenol. The H-ABS and ADD pathways will be investigated both theoretically and experimentally and correlated to the well-studied OH-promoted reaction of toluene. The results will allow to shed some light on the origin of the different regiochemistry in the NO_3-promoted nitration of these two aromatic compounds.

EXPERIMENTAL AND COMPUTATIONAL DETAILS

The reaction was studied in purified air at 760 Torr in a 480 L Teflon-coated 60 cm diameter cylindrical chamber equipped with an 81.2 m total beam path length White type mirror system coupled to a Bruker IFS 113V FT spectrometer for on-line Infrared Spectroscopy.

Concentrations of reactants and reaction products were monitored *in situ* by long path infrared spectroscopy. Experiments were performed at ambient pressure and temperature. Calibrations of the IR measurements were performed either by introducing known volumes of vapor at known pressures into the chamber or by evaporating known quantities of the compounds and transferring them with a stream of air into the chamber. Calibrated gas phase spectra of nitrotoluenes and nitrophenols were obtained.

NO_3 generated by reacting NO_2 with O_3 may be used as the promoter in gas phase nitration reactions.[24] The organic substrate is then admitted in the reactor and the nitration is due to the presence of NO_2 in the system. Moreover, the NO_3-initiated nitration of phenol with NO_2 in gas phase gives a ratio *ortho*:*para* which depends on the concentration of NO_2.[25]

In the experiments to study yields of nitrophenols, N_2O_5 was synthesized in the chamber by mixing O_3 with an excess of NO_2. Subsequently phenol was added and the reaction was allowed to proceed until only insignificant amounts (<100 ppb) of N_2O_5 remained. Initial concentrations were 10–25 ppmV N_2O_5, 3–55 ppmV NO_2, and 15–30 ppmV of the organic compound. In some experiments, phenol and NO_2 were added first to the chamber, then ozone. The initial concentrations in this case were 11–51 ppmV NO_2, 22–31 ppmV phenol and 16–70 ppmV ozone.

The rate constant of the reaction of NO_3 with phenols was determined relative to that of its reaction with 2-methyl-2-butene. In these experiments phenol and 2-methyl-2-butene were added first to the chamber, then N_2O_5 was introduced by evaporating solid N_2O_5, prepared by the method of Schott and Davidson,[26] and bringing it into the chamber with a stream of air. In this case, the initial concentrations were 15–18 ppmV of 2-methyl-2-butene and 5–10 ppmV phenol. N_2O_5 was in most experiments added several times during the experimental run in portions of a few ppmV. Initial NO_2 concentrations were 1–3 ppmV in these experiments. In other experiments, NO_2 was added to provide initial concentrations of 29–59 ppmV in order to test the influence of the concentration of NO_2 on the observed rate constant.

Structural parameters and energies of the reactants, intermediates and products along the H-ABS and ADD pathways of the NO_3-promoted nitration of toluene and phenol in their stable geometries and at transition states were computed in the framework of the density functional theory (DFT)[27] with the hybrid three parameter B3LYP[28,29] exchange-correlation functional and the split

Table 1. Distribution of nitration products from toluene and phenol in different conditions

	Toluene 1 (X = CH_2)		Phenol 1 (X = H)	
	NO_3-promoted nitration with NO_2[33]	Electrophilic[44]	NO_3-promoted nitration with NO_2[25]	Electrophilic[45]
Ortho-nitration	55	57	69–29	28
Meta-nitration	14	2		4
Para-nitration	31	41	40–17	58

valence basis set including a full set of polarization functions, 6-31G(d,p).[30] Minima and saddle-points (TS) of the potential energy were determined by gradient-based algorithms and by Synchronous Transit Guided Quasi-Newton (STQN) method.[31] The exact nature of each null-gradient point was checked by vibrational analysis. Free energy (G) values were calculated from the total partition function (Q), in which the terms $q_{translational}$, $q_{rotational}$, $q_{vibrational}$, are considered under the assumption that Q may be written as their product.[32] In order to evaluate enthalpy and entropy contributions, the value for temperature, and pressure was set to 298.15 K, and 1 Atm, respectively. Translations and rotations were treated classically and vibrational modes described according to the harmonic approximation.

RESULTS AND DISCUSSION

The NO_3-promoted nitration of toluene

In the NO_3-initiated gas phase nitration of toluene with NO_2 the distribution of reaction products is very similar to that occurring in the electrophilic nitration as shown in Table 1.[33] Again, ADD and H-ABS could occur, the former giving adducts **2–5** (X = CH_2; Y = NO_2) and consequently nitrotoluenes **15–17** (X = CH_2) via cyclohexadienes **8–14** (X = CH_2), the latter giving the benzyl radical **6** (X = CH_2) and then 4-nitrotoluene **15** (X = CH_2) and 2-nitrotoluene **16** (X = CH_2) (Schemes 1 and 2).

A kinetic isotope effect $k_H/k_D = 2.0–2.3$[34] was found and is close to the value of 1.5–1.8 found with *p*-xylene.[35] These values are borderline between being secondary and primary. A similar value ($k_H/k_D = 1.6$) was found for the reaction of toluene in acetonitrile with photochemically produced NO_3 and was attributed to an ET mechanism concerted with carbon–hydrogen bond cleavage to give a benzyl radical and a proton.[36]

In a LFER study the plot of log k for ten *para*-substituted toluenes *versus* Hammett's σ of the substituents gave $\rho = -4.3 \pm 0.6$; $r^2 = 0.87$.[37] This ρ value is more negative than that found in the reaction of OH with toluene ($\rho = -2.3 \pm 0.2$; $r^2 = 0.96$) and of that ($\rho = -3.2$) found in the reaction of toluenes substituted with electron-withdrawing groups with NO_3 in solution.[38] In both cases a rate-determining ADD mechanism was suggested. The H-ABS mechanism gives much lower ρ values. In fact, a ρ value of -0.72 was obtained[39] in the ozone-promoted nitration of phenols with NO_2 (the *Kyodai* nitration) occurring through a concerted addition-elimination pathway.

In order to settle the discrepancy between kinetic isotope effect and the LFER data the H-ABS and ADD reaction pathways were investigated theoretically and compared with the values calculated for the OH-initiated nitration of toluene. A detailed analysis of the theoretical results is presented elsewhere.[40] Here, we report only the values of the reaction (ΔG_r) and transition state ($\Delta G^{\#}$) free energy for the ADD and the H-ABS mechanism (Table 2).

Table 2. Reaction Gibbs free energy (ΔG_r; in kcal mol^{-1}) and corresponding transition state Gibbs free energy ($\Delta G^{\#}$; in kcal mol^{-1}) computed at **B3LYP**/6-31**G**(d,p) level of theory for the **OH**- and **NO_3**-promoted nitration of toluene and **NO_3**-promoted nitration of phenol

	Toluene		Phenol
	OH-promoted nitration	NO_3-promoted nitration	NO_3-promoted nitration
	ΔG_r	ΔG_r	ΔG_r
1 + OY→1-OY	−5.69	−5.76	−3.52
1-OY→6 + HOY **(H-ABS)**	−24.02	−6.97	−18.00
1-OY→2 **(ADD ipso)**	−8.94	7.20	5.58
1-OY→4 **(ADD** ortho**)**	−13.04	5.07	1.65
1-OY→3 **(ADD** meta**)**	−11.67	6.04	6.00
1-OY→5 **(ADD** para**)**	−13.72	5.13	4.43
	$\Delta G^{\#}$	$\Delta G^{\#}$	$\Delta G^{\#}$
1-OY→6-TS **(H-ABS)**	0.15	4.14	n.d.
1-OY→2-TS **(ADD ipso)**	2.63	10.72	11.21
1-OY→4-TS **(ADD** ortho**)**	0.99	8.83	8.18
1-OY→3-TS **(ADD** meta**)**	1.96	9.91	11.72
1-OY→5-TS **(ADD** para**)**	1.63	8.74	8.79

A pre-reactive complex between NO_3 and toluene (**1-NO_3**), corresponding to that reported by Vivier-Bunge *et al*.[6] for OH and toluene (**1-OH**), has been characterized by our calculations with a Gibbs free energy 5.76 kcal mol^{-1} lower than the separate reactants. This value is very similar (−5.69 kcal mol^{-1}) to that calculated for the OH-toluene complex at the same level of theory (Table 2).

The values of ΔG_r and $\Delta G^{\#}$ reported in Table 2 are referred to these pre-reactive complexes. In the NO_3-toluene complex the NO_3 radical is oriented perpendicular to the aromatic ring with two oxygen atoms pointing toward the ipso and *para* carbon atoms of toluene at a distance of 2.84 and 2.92 Å, respectively (Fig. 1). This NO_3-toluene pre-reactive complex can evolve to cyclohexadienes **2–5** (X = CH_2) through the ADD mechanism. It is interesting to note that addition of NO_3 to the four positions of the aromatic ring from the pre-reactive complex to form cyclohexadienes **2–5** (X = CH_2) is endoergonic by 5–7 kcal mol^{-1}, while the corresponding addition of OH to form cyclohexadienes **2–5** (X = OH) is significantly exoergonic (Table 2). In particular, in the case of the NO_3 + toluene reaction, the ΔG_r of the ADD pathways is within ±1 kcal mol^{-1} with respect to the separate reactants, while for the OH + toluene reaction, if the separate reactants are taken as reference, the addition pathway is still more exoergonic. The energy barriers ($\Delta G^{\#}$) for the addition of OH to the aromatic ring are positive and very low (within 1–3 kcal mol^{-1}; Table 2) if compared to the pre-reactive complex and negative if compared to the separate reactants. As discussed above this accounts for the positive slope of the Arrhenius plot observed for the rate of the OH decay at room temperature. On the other hand, $\Delta G^{\#}$ calculated for the NO_3 addition are still larger with respect to the separate reactants by 3–5 kcal mol^{-1}. The results presented above suggest that in the case of OH radical the pre-reactive complex evolves completely to give the

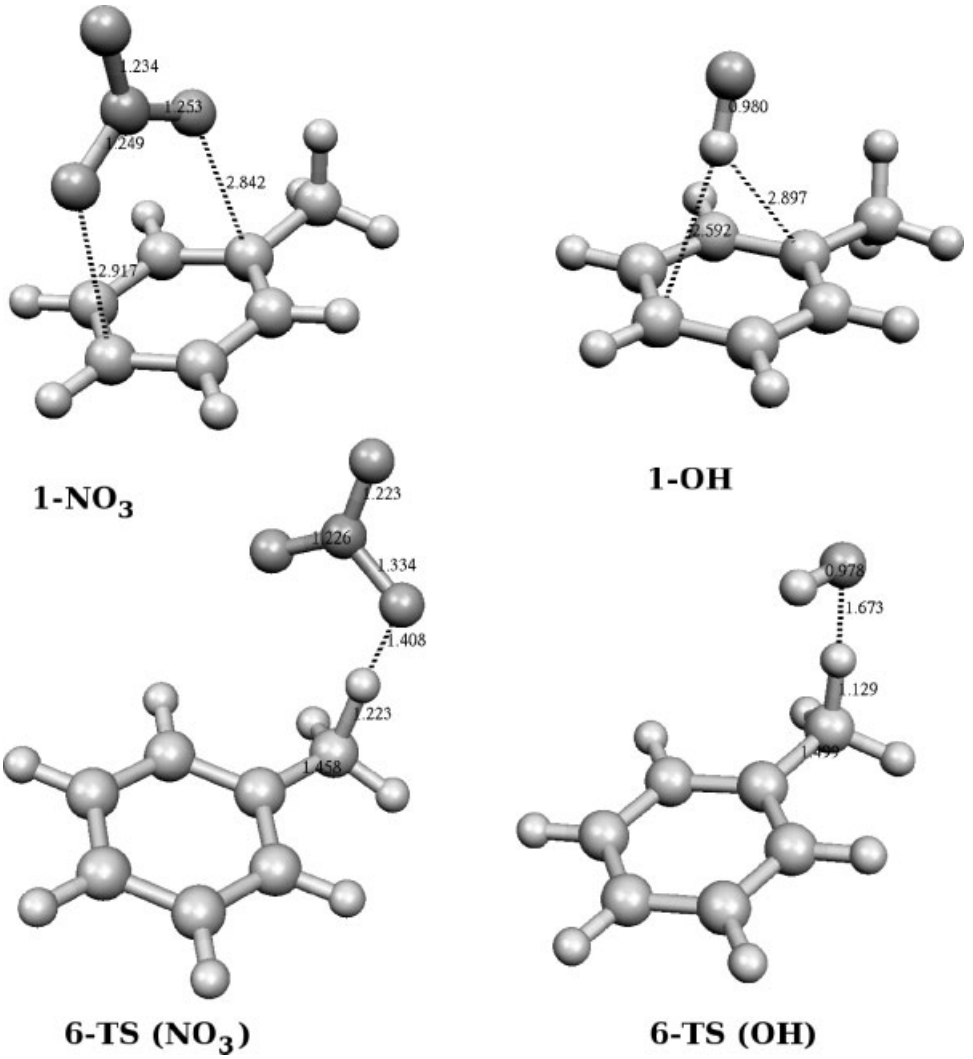

Figure 1. Selected geometry parameters of **1-NO_3** and **1-OH** complexes and of the corresponding transition states (**6-TS**) in the H-ABS mechanism computed at B3LYP/6-31G(d,p) level of theory

addition products, whereas in the case of NO_3 a significant amount of pre-reactive complex is present at the equilibrium.

As shown in Table 2, the H-ABS mechanism for the reactions of toluene with both OH and NO_3 is significantly more exoergonic than the corresponding ADD reaction. Furthermore, for the reaction of toluene with OH the $\Delta G^{\#}$ value of H-ABS is very similar to that of the ADD reaction, whereas for the NO_3 reaction the $\Delta G^{\#}$ value of H-ABS is significantly lower than that of the ADD reaction (Table 2). The geometry of the transition states (**6-TS**) (Fig. 1) is characterized by the NO_3 group far from the aromatic ring and with an oxygen atom in the C–H axis. The hydrogen atom to be transferred is at 1.223 and 1.408 Å from the carbon and oxygen atoms, respectively. An intrinsic reaction coordinate analysis (IRC) confirmed that **6-TS** is on the reaction coordinate which connects the pre-reactive complex to the reaction products. In the interpretation of the $\Delta G^{\#}$ values it should be noted that the B3LYP functional is well known to underestimate the energy barriers of hydrogen-transfer reactions by a few kcal mol^{-1}.[41] Furthermore, in the case of the ADD mechanism there are six different addition products which render this pathway statistically preferred. These considerations explain the great preference for the ADD pathway observed experimentally in the case of the addition of OH to toluene. In the case of NO_3 the reaction should proceed by a reversible ADD to give a mixture of cyclohexadienyl adduct and pre-reactive complex followed by the irreversible H-ABS step to give the benzyl radical final product. This mechanism is in line with the values of the Hammett's σ which refers to the reversible ring addition step and the kinetic isotope effect data which is related to the irreversible H-ABS step which leads to the final benzyl radical and HNO_3. Clearly, even if this latter mechanism is preferred, a fraction of the addition adducts (**2–5**) could react with NO_2 giving cyclohexadienes and consequently the final nitrotoluenes.

In order to further explore the regiochemistry of the NO_3-initiated nitration of toluene, we also investigated the final loss of nitric acid from the adducts **8–14**. In fact, even if the H-ABS pathway should be preferred to the ADD one, this latter mechanism can significantly contribute to the nitration reaction. Transition state energies for the elimination of HNO_3 from the cyclohexadienes **8–14** are collected in Table 3. All the cyclohexadienes having a *cis* arrangement of the groups to be eliminated (H and ONO_2) (e.g., in the *R*,*R* or *S*,*S* configuration) show transition state energies far lower than the corresponding *trans* isomers) (e.g., those in the *R*,*S* or *S*,*R* configuration). The transition state with *cis* intermediates shows early cleavage of the carbon–oxygen bond between the nitrate group and the ring carbon, thus suggesting that the loss of nitric acid from these intermediates is a concerted process[42] having a chair-like six-membered transition state.

Table 3. Transition state energies (kcal mol^{-1}) of the 1,2-elimination of HNO_3 to give nitrotoluenes computed at B3LYP/6-31G(d,p) level of theory

Cyclohexadiene	Configuration	By 1,2-elimination of HNO_3 gives	$\Delta E^{\#}$
(X = CH_2; Y = NO_2)			
8	*trans*	1,4-elimination	
8	*cis*	1,4-elimination	
9	1S,2R	**16**, *ortho*-nitrotoluene	60.49
9	1R,2R	**16**, *ortho*-nitrotoluene	16.34
12	2R,3R	**17**, *meta*-nitrotoluene	22.72
12	2S,3R	**17**, *meta*-nitrotoluene	60.58
13	2S,5R	1,4-elimination	
13	2R,5R	1,4-elimination	
10	2R,3R	**16**, *ortho*-nitrotoluene	23.43
10	2S,3R	**16**, *ortho*-nitrotoluene	62.63
11	3R,4R	**15**, *para*-nitrotoluene	20.75
11	3S,4R	**15**, *para*-nitrotoluene	61.29
14	3S,4R	**17**, *meta*-nitrotoluene	61.95
14	3R,4R	**17**, *meta*-nitrotoluene	21.90

The intermediates showing the lowest transition state energy for the loss of nitric acid (16.34 and 20.75 kcal mol^{-1}) predict for the formation of 2-nitrotoluene **16** (X = CH_2) and 4-nitrotoluene **15** (X = CH_2), which were the most abundant nitration products experimentally observed.

The NO_3-promoted nitration of phenol

In the NO_3-initiated gas phase nitration of phenol **1** (X = O) with NO_2 high yields of 2-nitrophenol **16** (X = O) are found. Also small amounts of 4-nitrophenol **15** (X = O) are formed and the ratio **16:15** (X = O) varies upon changing reaction conditions.

Concerning the reaction mechanism, phenol **1** (X = O) could undergo the ADD mechanism to give adducts **2–5** (X = O; Y = NO_2). Here, all isomeric nitrophenols should be formed. The isomerization of the ipso adduct **2** to intermediate **18** and then to 2-nitrophenol **16** (X = O) is also possible.

Alternatively, H-ABS to the phenoxy radical **6** (X = O) should give 4-nitrophenol **15** (X = O) and 2-nitrophenol **16** (X = O) exclusively.

The plot of log *k* for four *para*-substituted phenols *versus* Hammett's σ for the reaction with NO_3 gave $\rho = -1.48 \pm 0.89$; $r^2 = 0.79$, a value similar to that ($\rho = -1.0$) obtained in the reaction of the carbonate radical anion with phenol in solution to give phenoxy radicals via H-ABS.[43] However, H-ABS is unable to explain the predominant formation of the *ortho*-nitration product.

The experiments show that the ratio 2-nitrophenol **16** (X = O)/4-nitrophenol **15** (X = O) depends in this reaction from the initial ratio [NO_2]/[phenol] (Figs. 2 and

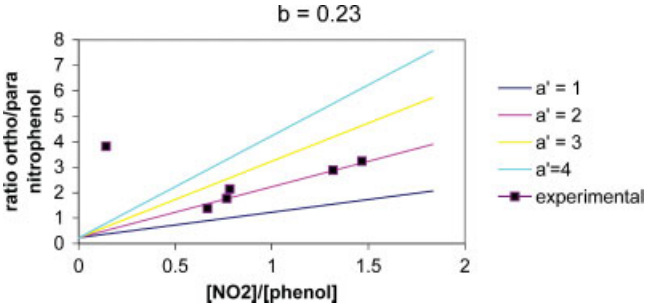

Figure 2. The dependence of the ratio 2-nitrophenol **16** (X = O)/4-nitrophenol **15** (X = O) from the ratio NO_2/phenol for $b = 0.23$

3, solid squares). To understand this fact, a kinetic analysis was performed.

The ipso radical adduct **2** and the *meta* radical adduct **3** (X = O) formed via k_{add} generate the final nitrophenols via three different pathways:

1. Slow addition of NO_2 via k_1 to give cyclohexadiene **9** (X = O) (from **2** X = O), or cyclohexadienes **10** and **11** (X = O) (from **3** X = O) followed by a fast irreversible elimination of nitric acid (k_{elim}). The formation of 2-nitrophenol **16** (X = O) from **9** (X = O) and of both 2–**16** and 4-nitrophenol **15** (X = O) (from **10** and **11** (X = O) is expected.
2. Loss of nitric acid via k_2 to form a phenoxy radical **6** (X = O) followed by reaction with NO_2 to give both 2-nitrophenol **16** (X = O) and 4-nitrophenol **15** (X = O) via k_{ortho} and k_{para}.
3. Isomerization of the ipso radical adduct **2** via k_3 with formation of intermediate **18** and then of 2-nitrophenol **16** (X = O) exclusively.

The steady state hypothesis was applied to intermediates **2**, **3**, **6**, **9**, **10**, and **11** according to Scheme 3. Since initial values of [phenol] and [NO_2] are much higher than the partial pressures of the products found at the end of the experiment, they can be considered as constant. In other words, the values v_{ortho} and v_{para} actually measured by

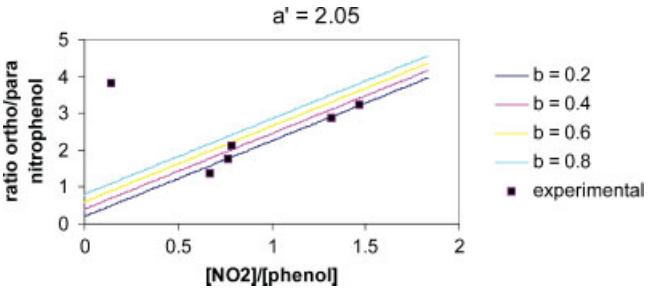

Figure 3. Simulated dependence of the ratio 2-nitrophenol 16 (X = O)/4-nitrophenol 15 (X = O) from the ratio NO_2/phenol for $a' = 2.05$

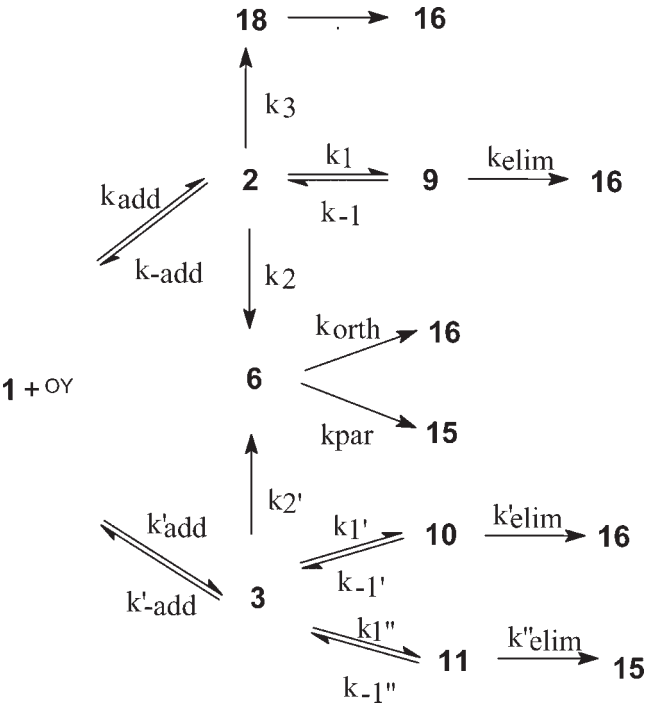

Scheme 3

determining the content of 2-nitrophenol **16** (X = O) and 4-nitrophenol **15** (X = O) of the reaction mixture are initial rates, $(v_{ortho})_0$ and $(v_{para})_0$. The initial rates are correlated to the initial values of partial pressures of reactants, $[phenol]_0$ and $[NO_2]_0$, respectively. In this case the ratio between 2-nitrophenol **16** and 4-nitrophenol **15** can be estimated as the ratio between $(v_{ortho})_0$ and $(v_{para})_0$. This ratio is a linear function of $[NO_2]_0$. It may be shown that:

$$[2-\text{nitrophenol } \mathbf{16}]/[4-\text{nitrophenol } \mathbf{15}]$$
$$= (v_{ortho})_0/(v_{para})_0 = a[NO_2]_0 + b$$

where a and b are complex combinations of the rate constant involved (see supplementary material).

Five values of the ratio 2-nitrophenol **16** (X = O)/4-nitrophenol **15** (X = O) shown in Figs. 2 and 3 give $a = 2.06$ and $b = 0.23$. Hence, the increase in the ratio 2-nitrophenol **16** (X = O)/4-nitrophenol **15** (X = O) reflects the increased importance of pathway 2 (reaction via a phenoxy radical **6** (X = O) with consequent loss of regiochemistry) over pathway 1 (reaction via a cyclohexadiene with consequent control of the stereochemistry). The ratio [NO_2]/[phenol] controls the slow step in pathway 1 but not the loss of nitric acid in pathway 2. Increasing this ratio from 0.67 to 1.46 results in a higher amount of NO_2 available for the bimolecular process constituting the slow step in pathway 1, thus allowing this pathway to compete with pathway 2.

A different situation occurs when the ratio [NO_2]/[phenol] is as low as 0.14. Here, *ortho*-nitration sharply predominates, indicating that the ADD pathway is

preferred to H-ABS. The low concentration of NO_3 in these conditions could switch part of the ipso adduct **2** to isomerization to **18** and consequently to the formation of the *ortho* nitration product. In other words k_3 (Scheme 3) could compete with k_2 in these conditions.

The H-ABS and ADD pathways of the NO_3-initiated nitration of phenol were also investigated theoretically and correlated to the experimental data. A pre-reactive NO_3-phenol complex, similar to that described above for toluene has been found with a Gibbs free energy about 3.5 kcal mol^{-1} lower than the separate reactants (Table 2). As noted for toluene, the NO_3-phenol pre-reactive complex can evolve to the cyclohexadienes **2–5** (X = OH) through the ADD mechanism. This process is endoergonic by about 2 kcal mol^{-1} with respect to the separate reactants for the ipso, *meta*, and *para* addition. For the *ortho* addition the process is exoergonic by about 2 kcal mol^{-1}. The larger stability of the *ortho*- with respect to the ipso, *meta*, and *para* adducts is due to the formation of a hydrogen bond between an oxygen atom of the NO_3 group and the hydrogen atom of the hydroxyl group. $\Delta G^{\#}$ are similar to those calculated for the ADD mechanism of toluene. In this case, due to the lower ΔG_r of the pre-reactive complex, $\Delta G^{\#}$ are about 5–7 kcal mol^{-1} larger than the separate reactants, values slightly larger than that calculated for the NO_3-toluene system. These results suggest that at the equilibrium the yield of pre-reactive complex is significantly larger than that of the adducts. On the other hand, the H-ABS mechanism is significantly exoergonic (Table 2) suggesting a preferred and irreversible formation of the phenoxy radical. However, we were not able to locate a TS along the reaction coordinate connecting the pre-reactive complex and the H-ABS products. This should be explained by considering the great distance between the hydrogen atom of the OH group, which, in the pre-reactive complex, is in the plane of the aromatic ring, and the oxygen atom of the NO_3 radical. In fact, differently from toluene, at the transition state **6-TS** bond formation should involve a significant rotation of the C—OH bond. Therefore, the formation of the pre-reactive complex should selectively drive the reaction toward the ADD mechanism. On the other hand, the H-ABS process should involve a less probable mechanism in which the reaction coordinate start from the two separate reactants. In summary, the comparison between these two pathways suggest that the ADD mechanism is preferred over H-ABS. Based on the results considered above the regiochemistry of the NO_3-initiated nitration of phenol should be explained by considering the irreversible elimination of HNO_3 from the **8–14** adducts.

Activation energy values of this latter process are reported in Table 4. The transition state energy from the elimination of nitric acid from these was calculated as above. Again, all the cyclohexadienes having a *cis* arrangement of the groups to be eliminated (H and ONO_2) (e.g., in the *R*,*R* or *S*,*S* configuration) show transition state energies far lower than the corresponding trans isomers) (e.g., those in the *R*,*S* or *S*,*R* configuration). Again, the transition state with *cis* intermediates shows early cleavage of the carbon–oxygen bond between the nitrate group and the ring carbon, thus suggesting that the loss of nitric acid is a concerted process[25] having a chair-like six-membered transition state. Cyclohexadiene **9**, (X = O; Y = NO_2, 1R,2R), shows the lowest transition state energy for the loss of nitric acid (12.40 kcal mol^{-1}) and predicts the preferential formation of 2-nitrophenol **16** (X = O).

Table 4. Transition state energies (kcal mol^{-1}) of the 1,2-elimination of HNO_3 to give nitrophenols computed at B3LYP/6-31G(d,p) level of theory

Cyclohexadiene	Configuration	By 1,2-elimination of HNO_3 gives	$\Delta E^{\#}$
(X = CH_2; Y = NO_2)			
8	*trans*	1,4-elimination	
8	*cis*	1,4-elimination	
9	1R,2R	**16**, *ortho*-nitrophenol	12.40
9	1S,2R	**16**, *ortho*-nitrophenol	54.47
12	2S,3R	**17**, *meta*-nitrophenol	23.20
12	2R,3R	**17**, *meta*-nitrophenol	65.30
13	2R,4R	1,4-elimination	
13	2S,4R	1,4-elimination	
10	2S,3R	**16**, *ortho*-nitrophenol	18.19
10	2R,3R	**16**, *ortho*-nitrophenol	56.14
11	3S,4R	**15**, *para*-nitrophenol	61.36
11	3R,4R	**15**, *para*-nitrophenol	17.40
14	3S,4R	**17**, *meta*-nitrophenol	63.30
14	3R,4R	**17**, *meta*-nitrophenol	24.81

CONCLUSIONS

In conclusion the NO_3-promoted nitration of toluene in presence of NO_2 occurs mostly via a rate-determining H-ABS process. The H-ABS step is preceded by an equilibrium between the pre-reactive complex and the addition adducts, therefore accounting for the values of the Hammett's σ which appear to indicate an ADD mechanism. The ADD mechanism should also be operative to a lesser extent and the preference for the nitration in *ortho* and *para* position, in this case, should depend from the concerted loss of nitric acid from the intermediate cyclohexadienes. The NO_3-promoted nitration of phenol in presence of NO_2 occurs mostly via a rate-determining ADD mechanism and the stereocontrolled elimination of nitric acid has an important role in driving the reaction toward the *ortho*-nitration. The reasons for the dependence of the ratio *ortho*:*para*-nitration from the initial concentration of reactants are understood. These observations may be useful for modeling the chemistry in the tropospheric gas phase.

REFERENCES

1. Finlayson-Pitts BJ, Pitts N. *Atmospheric Chemistry: Fundamentals and Experimental Techniques*. Wiley Interscience: New York, 1986.
2. Calvert JG, Atkinson R, Becker KH, Kamens RM, Seinfeld JH, Wallington TJ. *The Mechanism of Atmospheric Oxidation of Aromatic Hydrocarbons*Yarwood G (ed.). Oxford University Press: Oxford, 2002.
3. Perry RA, Atkinson R, Pitts JN. *J. Phys. Chem*. 1977; **81**: 286–304.
4. Kenley RA, Davenport JE, Hendry DG. *J. Phys. Chem*. 1981; **85**: 2740–2746.
5. Singleton DL, Cvetanovic RJ. *J. Am. Chem. Soc*. 1976; **98**: 6812–6819.
6. Uc VH, García-Cruz I, Hernández-Laguna A, Vivier-Bunge A. *J. Phys. Chem A* 2000; **104**: 7847–7855.
7. Atkinson R, Lloyd AC. *J. Phys. Chem. Ref. Data* 1984; **3**: 3155–3444.
8. Klotz B, Sorensen S, Barnes I, Becker KH, Etzkorn T, Volkamer R, Platt U, Wirtz K, Martin Reviejo J. *J. Phys. Chem. A*. 1998; **102**: 10289–10299.
9. Suzuki H, Murashima T, Kozai I, Mori T. *J. Chem. Soc. Perkin Trans 1*, 1993; 1591–1596.
10. (a) Andino JM, Smith JN, Flagan RC, Goddard WAIII, Seinfeld JH. *J. Phys. Chem*. 1996; **100**: 10967–10980; (b) Lay TH, Bozzelli JW, Seinfeld JH. *J. Phys. Chem*. 1996; **100**: 6543–6554.
11. (a) Atkinson R. *J. Phys. Chem. Ref. Data, Monograph 1*, 1989; (b) Atkinson R, Ashmann SM. *Int. J. Chem. Kinet*. 1988; **20**: 513–518.
12. Bolzacchini E. Hjorth J. Meinardi S. Orlandi M. Restelli G. Rindone B. In *Free Radicals in Biology and the Environment*, Minisci F (ed.). Kluwer Academic Press: The Netherlands, 1997, 409–422.
13. Wiberg KB, Slaugh LH. *J. Am. Chem. Soc*. 1958; **80**: 3033–3039.
14. Hanzlik RP, Hogberg K, Moon JB, Judson CM. *J. Am. Chem. Soc*. 1985; **107**: 7164–7167.
15. van Helden R, Kooijman EC. *Recueil des Travaux Chimiques des Pays-Bas et de la Belgique* 1954; **73**: 269–278.
16. Fonouni HE, Krishnan S, Kuhn DG, Hamilton GA. *J. Am. Chem. Soc*. 1983; **105**: 7672–7676.
17. Hanzlik RP, Schaefer AR, Moon JB, Judson CM. *J. Am. Chem. Soc*. 1987; **109**: 4926–4930.
18. Nakano T, Kawabata S, Sugihara T, Agatsuma N, Kakuda H, Mori Y. *Bull. Chem. Soc. Jpn* 2003; **76**: 2353–2360.
19. (a) Bohn B. Zetzsch C. *Phys. Chem. Chem. Phys*. 1999; **1**: 5097–5107; (b) Chen C-C, Bozzelli JW, Farrell JT, Johnson D, Raoulr S, Rayez MT, Rayez J-C, Lesclaux R. *Phys. Chem. Chem. Phys*. 2002; **4**: 4678–4686; (c) Ghigo G, Motta F, Tonachini G. *Recent Res. Dev. Org. Chem.* 2002; **6**: 129–145; (d) Grebenkin S, Krasnoperov LN. *J. Phys. Chem. A* 2004; **108**: 1953–1963, 4632–4652.
20. Atkinson R, Aschmann S, Arey J, Carter W. *Int. J. Chem. Kinet*. 1989; **21**: 801–812.
21. See in particular reference 8.
22. Klotz B, Barnes I, Becker KH. *Int. J. Chem. Kinet*. 1999; **31**: 689–697.
23. Knispel R, Roch R, Siese M, Zetzsch C. *Berichte der Bunsen Gesellschaft* 1990; **94**: 1375–1379.
24. Wayne RP, Barnes I, Biggs P, Burrows JP, Canosa-Mas CE, Hjorth J, LeBras G, Moortgat KG, Perner D, Polet G, Restelli G, Sidebottom H. *Atmos. Environm* 1991: **25**: 1–206.
25. (a) Bolzacchini E, Bruschi M, Hjorth J, Meinardi S, Orlandi M, Rindone B, Rosenbohm E. *Environ. Sci. Technol*. 2001; **35**: 1791–1797; (b) Barzaghi P, Herrmann H. *Phys. Chem. Chem. Phys*. 2002; **4**: 3669–3675.
26. Schott G, Davidson N*J. Am. Chem. Soc*. 1958; **80**: 1841–1853.
27. Parr RG, Yang W. In *Density Functional Theory of Atoms and Molecules*. Oxford University Press: New York, 1989.
28. Becke AD. *J. Chem.Phys*. 1993; **98**: 5648–5652.
29. Lee C, Yang W, Parr R. *G. Phys. Rev. B* 1988, **37**: 785–789.
30. Frisch MJ, Trucks GW, Schlege HB, Gill PMW, Johnson BG, Robb MA, Cheeseman JR, Keith TA, Petersson GA, Montgomery JA, Raghavachari K, Al-Laham MA, Zakrzewski VG, Ortiz JV, Foresman JB, Cioslowski J, Stefanov BB, Nanayakkara A, Challacombe M, Peng CY, Ayala PY, Chen W, Wong MW, Andres JL, Replogle ES, Gomperts R, Martin RL, Fox DJ, Binkley JS, Defrees DJ, Beker J, Stewart JP, Head-Gordon M, Gonzales G, Pople JA. *Gaussian 94*. Gaussian, Inc: Pittsburgh, PA, 1995.
31. (a) Peng C, Schlegel HB. *Israel J. Chem*. 1994; **33**: 449–454; (b) Peng C, Ayala PJ, Schlegel HB, Frisch MJ. *J. Comp. Chem*. 1996; **17**: 49–56.
32. Jensen F*Introduction to Computational Chemistry.* John Wiley & Sons Ltd: Baffins Lane, Chichester, England.
33. Chiodini G, Rindone B, Polesello S, Cariati F, Hjorth J, Restelli G. *Environ. Sci. Technol* 1993; **27**: 1659–1664.
34. Atkinson R, Aschmann S. *Int. J. Chem. Kinet.* 1988; **20**: 513–539.
35. Rindone B, Cariati F, Restellli G, Hjorth J. *Fresenius J. Anal. Chem*. 1991; **339**: 673–675.
36. (a) Ito O, Seiji A, Iino M. *J. Org. Chem*. 1989; **54**: 2436–2440; (b) Del Giacco T, Baciocchi E, Steenken S. *J. Phys. Chem*. 1993; **97**: 5451–5456.
37. Bolzacchini E, Meinardi S, Orlandi M, Rindone B, Hjorth J, Restelli G. *Environ. Sci. Technol*. 1999; **33**: 461–468.
38. Ito O, Akhido S, Iino M. *J. Org. Chem*. 1989; **54**: 2436–2440.
39. Barletta B, Bolzacchini E, Meinardi S, Orlandi M, Rindone B. *Environ. Sci. Technol*. 2000; **34**: 2224–2230.
40. Submitted to *J. Phys. Chem. A*.
41. (a) Lynch BJ, Truhlar DG. *J. Phys. Chem. A* 2001; **105**: 2936–2941; (b) Tordini F, Bencini A, Bruschi M, De Gioia L, Zampella G, Fantucci P. *J. Phys. Chem A* 2003; **107**: 1188–1196.
42. Bolzacchini E, Meinardi S, Orlandi M, Rindone B, Hjorth J, Restelli G. *Environ. Sci. Technol*. 1999, **33**: 461–468.
43. Moore JS, Phillips GO, Sosnowski A. *Int. J. Rad. Biol. Relat. Stud. Phys. Chem. Med.* 1977; **31**: 603–605.
44. Suzuki H, Murashima T, Kozai I, Mori T. *J. Chem. Soc. Perkin Trans 1*, 1993; 1591–1596.
45. Olah GA, Malhotra R, Narang SC. *Nitration: Methods and Mechanism.* VHC Publishers Inc: New York, 1989; 201–204.